REVIEW SUMMARY

CLIMATE VARIABILITY

Decadal climate variability in the tropical Pacific: Characteristics, causes, predictability, and prospects

Scott Power*, Matthieu Lengaigne, Antonietta Capotondi, Myriam Khodri, Jérôme Vialard, Beyrem Jebri, Eric Guilyardi, Shayne McGregor, Jong-Seong Kug, Matthew Newman, Michael J. McPhaden, Gerald Meehl, Doug Smith, Julia Cole, Julien Emile-Geay, Daniel Vimont, Andrew T. Wittenberg, Mat Collins, Geon-Il Kim, Wenju Cai, Yuko Okumura, Christine Chung, Kim M. Cobb, François Delage, Yann Y. Planton, Aaron Levine, Feng Zhu, Janet Sprintall, Emanuele Di Lorenzo, Xuebin Zhang, Jing-Jia Luo, Xiaopei Lin, Magdalena Balmaseda, Guojian Wang, Benjamin J. Henley

BACKGROUND: Tropical Pacific decadal climate variability and change (TPDV) affects the global climate system, extreme weather events, agricultural production, streamflow, marine and terrestrial ecosystems, and biodiversity. Although major international efforts are underway to provide decadal climate predictions, there is still a great deal of uncertainty about the characteristics and causes of TPDV and the accuracy to which it can be simulated and predicted. Here, we critically synthesize what, as of now, is known and not known and provide recommendations to improve our understanding of TPDV and our ability to predict it.

ADVANCES: TPDV is evident in instrumental records, paleoclimate records over past millennia, and climate models. TPDV can occur spontaneously as "internal" variability, as is largely the case in the central equatorial Pacific, or in response to "external" forcing. Although internal TPDV arises to a large extent as a residual of independent El Niño–Southern Oscillation (ENSO) events, it can also result from oceanic processes occurring at decadal time scales involving the upper-ocean overturning circulation known as subtropical-tropical cells and in response to internal atmospheric variability in the extra-tropical Pacific and changes in sea surface temperature in other ocean basins. Externally forced TPDV, in the form of mean-state changes that unfold on decadal time scales or forced decadal variability, can be driven by anthropogenic [e.g., greenhouse gas (GHG) increases, sulfate aerosols changes] and natural processes (e.g., volcanic eruptions). External forcing can also affect the behavior and characteristics of internal TPDV.

In the western tropical Pacific, GHG-forced warming has reached levels that are unprecedented in the historical record. Further greenhouse warming in the equatorial Pacific will ensure that record-setting high temperatures will be experienced for decades to come. Increases in equatorial precipitation and in precipitation variability in parts of the tropical Pacific, and a southward expansion of the southern hemisphere Hadley cell, are projected by climate models with some confidence. Yet projected changes in eastern equatorial Pacific surface temperature, and changes in the strength of the Walker circulation and trade winds, remain very uncertain.

Skill in decadal predictions of temperature in the western Pacific is apparent, though it appears to be largely underpinned by GHG warming. There are also indications of multiyear skill in predicting some biogeochemical quantities important for fisheries and the global carbon budget.

The limited length of the instrumental records, the scarcity of paleoclimate data, and TPDV representation biases in climate models have so far prevented a complete characterization and understanding of TPDV. These issues have also limited our ability to predict TPDV.

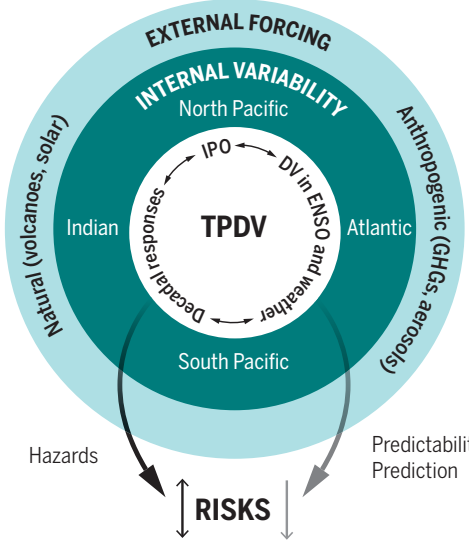

Schematic overview of key issues raised. The inner circle provides a few examples of TPDV, together with some of the processes responsible for TPDV originating in the tropical Pacific. These include the Interdecadal Pacific Oscillation (IPO), decadal responses to external forcing, decadal variability in ENSO and weather, and the impact of this decadal variability on the tropical Pacific. The small, two-way arrows in the inner circle indicate the possibility of two-way interactions between these phenomena. The inner ring describes internal processes that can drive or influence TPDV, indicating that this can originate in the Pacific beyond the tropical Pacific and in the (tropical) Indian and Atlantic Oceans. The outer ring represents external forcing that can drive or influence TPDV. This includes both natural (e.g., volcanoes) and anthropogenic (e.g., anthropogenic GHG emissions) factors. The large arrows extending to the bottom of the figure represent the risks associated with TPDV (e.g., drought). The arrow on the left indicates that TPDV affects such risks. The arrow is dark to indicate that many of the risks are well established. The large arrow on the right indicates that skillful predictions, which depend on the existence of predictability in the climate system, can help to reduce the risks. This arrow is gray to indicate that decadal predictions for the tropical Pacific are still at a formative stage.

OUTLOOK: Although several mechanisms have been proposed to explain TPDV, their relative importance as sources of decadal prediction remains unclear. Issues in need of greater understanding include the role played by the upper ocean overturning circulation in controlling tropical Pacific sea surface temperatures at decadal time scales, the impact of external forcing on the Walker circulation and characteristics of internally generated TPDV, and the extent to which sea surface temperature variability in other basins drives TPDV. A better understanding of the origin and spatial pattern of current predictive skill is also needed. Improving predictions and projections requires improvements in the quality, quantity, and length of instrumental and paleoclimate records and in the performance of climate models and data assimilation methods used to make predictions. ■

The list of author affiliations is available in the full article online.
*Corresponding author. Email: scott.power@usq.edu.au
Cite this article as S. Power *et al.*, *Science* **374**, eaay9165 (2021). DOI: 10.1126/science.aay9165

FULL ARTICLE https://doi.org/10.1126/science.aay9165

REVIEW

CLIMATE VARIABILITY

Decadal climate variability in the tropical Pacific: Characteristics, causes, predictability, and prospects

Scott Power[1,2,3]*, Matthieu Lengaigne[4], Antonietta Capotondi[5,6], Myriam Khodri[7], Jérôme Vialard[7], Beyrem Jebri[7], Eric Guilyardi[7,8], Shayne McGregor[2], Jong-Seong Kug[9], Matthew Newman[5,6], Michael J. McPhaden[10], Gerald Meehl[11], Doug Smith[12], Julia Cole[13], Julien Emile-Geay[14], Daniel Vimont[15], Andrew T. Wittenberg[16], Mat Collins[17], Geon-Il Kim[9], Wenju Cai[18,19,20], Yuko Okumura[21], Christine Chung[22], Kim M. Cobb[23], François Delage[22], Yann Y. Planton[10], Aaron Levine[10], Feng Zhu[21], Janet Sprintall[24], Emanuele Di Lorenzo[25], Xuebin Zhang[18], Jing-Jia Luo[26], Xiaopei Lin[19,20], Magdalena Balmaseda[27], Guojian Wang[18], Benjamin J. Henley[2,3,28]

Climate variability in the tropical Pacific affects global climate on a wide range of time scales. On interannual time scales, the tropical Pacific is home to the El Niño–Southern Oscillation (ENSO). Decadal variations and changes in the tropical Pacific, referred to here collectively as tropical Pacific decadal variability (TPDV), also profoundly affect the climate system. Here, we use TPDV to refer to any form of decadal climate variability or change that occurs in the atmosphere, the ocean, and over land within the tropical Pacific. "Decadal," which we use in a broad sense to encompass multiyear through multidecadal time scales, includes variability about the mean state on decadal time scales, externally forced mean-state changes that unfold on decadal time scales, and decadal variations in the behavior of higher-frequency modes like ENSO.

Naturally occurring, spontaneously generated tropical Pacific decadal variability (TPDV) like the El Niño–Southern Oscillation (ENSO), the most energetic and influential climate phenomenon in the world (*1*), can arise in the absence of any change to external forcing [e.g., greenhouse gas (GHG) increases or volcanic eruptions]. Climate scientists refer to such variability as "internally generated" or "internal" variability, and it will be referred to here as "internal TPDV" (*2*). Internal TPDV affected the rate at which globally averaged surface air temperature rose over the past century. This was dramatically illustrated by the recent and highly publicized "global warming slowdown," when decadal surface cooling in the eastern equatorial Pacific (shading in Fig. 1A) associated with a major redistribution of heat in the subsurface ocean offset the anthropogenic global warming trend at the turn of the 21st century (*3*, *4*) (bottom black curve in Fig. 1D). Trade wind intensification associated with this cooling also contributed to rapid sea level rise in the western Pacific during recent decades (*5*) (contours in Fig. 1A). More generally, internal TPDV has further been reported to modulate drought; wildfire; floods; extreme weather; polar sea ice extent (*6*, *7*); decadal variations in the impact that ENSO has on rainfall, river flow, and agricultural production; and the skill with which ENSO impacts can be predicted, as demonstrated for Australia (*8*). Uncertainty in the magnitude of internal TPDV simulated in global climate models may also be linked to uncertainty in simulated climate sensitivity (*9*)—a measure of the degree of global warming that occurs in response to anthropogenic increases in atmospheric GHG concentrations (*10*).

The tropical Pacific also changes in response to external forcing, including GHG increases, volcanic eruptions, and anthropogenic aerosols. This component of TPDV will be referred to as "external TPDV." The observed low-frequency sea surface temperature (SST) evolution over the western tropical Pacific warm pool is dominated by a long-term warming trend similar to the global anthropogenic warming signal (bottom black curves in Fig. 1D) that has been linked to a drying trend in the East Asian monsoon (*11*). Further warming in the region is also expected to reduce coastal fish populations, shift tuna distribution eastward, cause record-breaking high temperatures to occur more often (*12*), and fundamentally alter coral reefs, with major impacts on biodiversity, Pacific Island communities, and livelihoods (*12*, *13*).

Major international efforts are underway to provide decadal climate predictions that are intended to help decision-makers plan for the coming years and decades (*14*); these efforts take both internally generated and externally forced TPDV into account, because they will both influence future climate. The enormous challenges now faced by groups that produce decadal predictions demand a better understanding of the mechanisms of TPDV. To that end, here we synthesize our current understanding of TPDV, its spatial and temporal characteristics, its many proposed mechanisms—both natural and anthropogenic and the interactions between them—and the current ability of state-of-the-art modeling and prediction systems to simulate and predict TPDV. A wide and diverse array of evidence is used—including historical records, instrumental and paleoclimate observations, mathematical models of Earth's climate, and decadal prediction systems—to assess the degree of confidence that we have in proposed mechanisms and the extent to which those processes provide a degree of predictability (*2*, *14*, *15*).

Advances

Observed TPDV

Decadal SST fluctuations peak in the equatorial central and eastern Pacific (contours in Fig. 1B), alternating between decadal periods of anomalously warm and cold phases (top black curve in Fig. 1D). This evolution broadly matches the positive and negative phases of the Interdecadal Pacific Oscillation (*8*) (represented as vertical shading in Fig. 1D), characterized by opposite SST and sea level signals in

[1]Centre for Applied Climate Sciences, University of Southern Queensland, Toowoomba, QLD, Australia. [2]School of Earth, Atmosphere, and Environment, Monash University, Clayton, VIC, Australia. [3]ARC Centre of Excellence for Climate Extremes, Monash University, Clayton, VIC, Australia. [4]MARBEC, University of Montpellier, CNRS, IFREMER, IRD Sète, Montpellier, France. [5]Cooperative Institute for Research in Environmental Sciences, University of Colorado, Boulder, CO, USA. [6]Physical Sciences Laboratory, NOAA, Boulder, CO, USA. [7]LOCEAN-IPSL, Sorbonne Universités/UPMC/CNRS/IRD/MNHN, Paris, France. [8]National Centre of Atmospheric Science, University of Reading, Reading, UK. [9]Division of Environmental Science and Engineering, Pohang University of Science and Technology (POSTECH), Pohang, South Korea. [10]NOAA–Pacific Marine Environmental Laboratory, Seattle, WA, USA. [11]National Center for Atmospheric Research, Boulder, CO, USA. [12]Met Office Hadley Centre, Exeter, UK. [13]Department of Earth and Environmental Sciences, University of Michigan, Ann Arbor, MI, USA. [14]Department of Earth Sciences, University of Southern California, Los Angeles, CA, USA. [15]Atmospheric and Oceanic Science, University of Wisconsin–Madison, Madison, WI, USA. [16]NOAA Geophysical Fluid Dynamics Laboratory, Princeton, NJ, USA. [17]College of Engineering, Mathematics and Physical Sciences, University of Exeter, Exeter EX4 4QE, UK. [18]Centre for Southern Hemisphere Oceans Research, CSIRO Oceans and Atmosphere, Hobart, TAS 7001, Australia. [19]Frontier Science Center for Deep Ocean Multispheres and Earth System and Laboratory of Physical Oceanography, Ocean University of China, Qingdao, China. [20]Qingdao National Laboratory for Marine Science and Technology, Qingdao 266003, China. [21]Institute for Geophysics, Jackson School of Geosciences, The University of Texas at Austin, Austin, TX, USA. [22]Bureau of Meteorology, Docklands, VIC, Australia. [23]School of Earth and Atmospheric Sciences, Georgia Institute of Technology, Atlanta, GA, USA. [24]Scripps Institution of Oceanography, University of California, San Diego, La Jolla, CA, USA. [25]Program in Ocean Science & Engineering, Georgia Institute of Technology, Atlanta, GA, USA. [26]Institute for Climate and Application Research (ICAR)/CICFEM/KLME/ILCEC, Nanjing University of Information Science and Technology, Nanjing, China. [27]European Centre for Medium-Range Weather Forecasts, Reading, UK. [28]Securing Antarctica's Environmental Future, Monash University, Clayton, VIC, Australia.
*Corresponding author. Email: scott.power@usq.edu.au

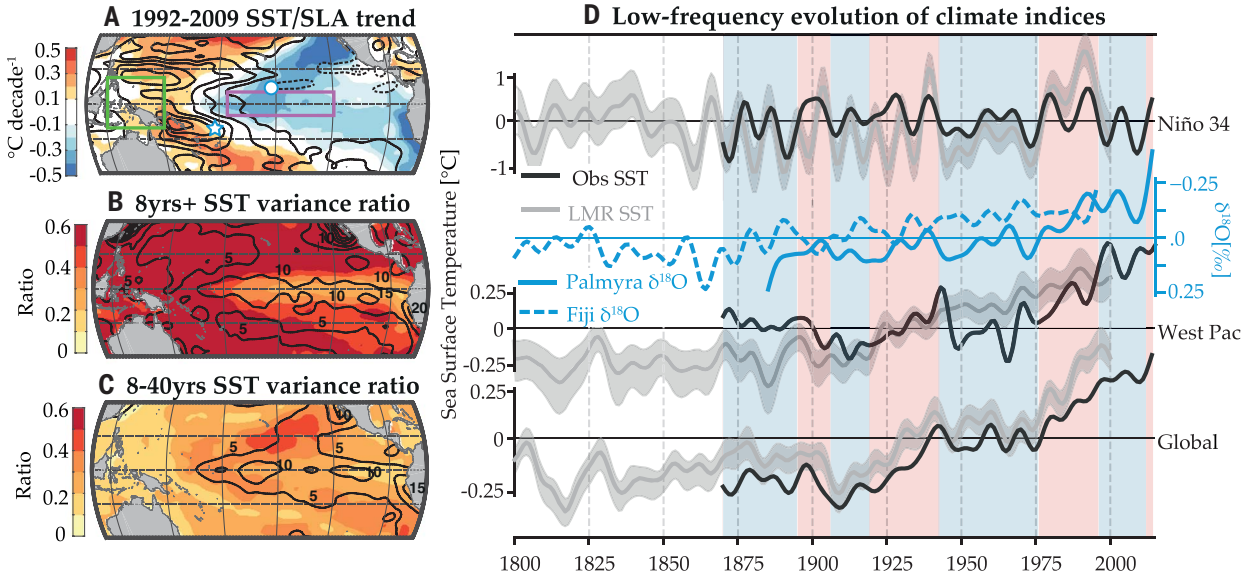

Fig. 1. Observed decadal variability in the tropical Pacific. (**A**) 1992–2009 linear trend of annual SST (shading, 0.1°C decade^{-1}) and sea surface height (black contours, 2 cm decade^{-1}, where dashed contours indicate negative trends, solid contours indicate positive trends, and the zero contour is omitted). (**B** and **C**) Eight-year low-pass (B) and 8- to 40-year band-pass (C) filtered SST variance (black contours, in 10^2 °C^2) and ratio of the filtered SST variance to total SST variance (shading). (**D**) Eight-year low-pass filtered time series of SST averaged over the Niño34 region (5°N to 5°S; 170°W to 120°W), over the western tropical Pacific (10°N to 10°S; 120°E to 150°E), and over the globe from instrumental observations (Obs, black lines) and Last Millennium Reconstruction (LMR) [(*19*); the gray line indicates the mean, and the light gray shading indicates the interquartile range] and of $\delta^{18}O$, a measure of the ratio of stable isotopes oxygen-18 and oxygen-16, at Palmyra and Fiji islands [plain and dashed blue lines; positions indicated in (A); (*17*, *18*)]. Vertical red and blue bands indicate positive and negative phases of the Interdecadal Pacific Oscillation, respectively. SST data: Hadley Centre Sea Ice and Sea Surface Temperature (HadISST) (*96*). SSH data: Ocean Reanalysis System 4(ORAS4) dataset (*97*).

the eastern and western tropical Pacific (Fig. 1A). Although important on decadal time scales, this variability only modestly contributes to total SST variations in the equatorial eastern Pacific (shading in Fig. 1B), which are largely dominated by ENSO-related interannual SST fluctuations. The relative contribution of TPDV is considerably larger in the western Pacific, where the low-frequency SST signal is dominated by a long-term warming trend similar to the global anthropogenic warming signal (bottom black curves in Fig. 1D). Consequently, internal TPDV, estimated here in the 8- to 40-year range, dominates in the central Pacific and in off-equatorial bands in the eastern part of the basin, especially in the Northern Hemisphere. Internal TPDV has a weak signature in the western tropical Pacific (Fig. 1C), where the longer time scales of external TPDV prevail instead.

Confidently characterizing TPDV is complicated by the short historical record. Indeed, historical observations of the tropical Pacific are sparse before the mid-20th century, which creates uncertainty in tropical Pacific SST records before 1950. Paleoclimate records offer key complementary information extending further into the past (Fig. 1D). A recent synthesis of dozens of monthly to annually resolved Pacific coral records exhibits strong decadal variability over the past four centuries (*16*). In particular, isotopic measurements from corals in the central and southwest tropical Pacific (*17*, *18*) (white dot and star in Fig. 1A) display a monotonic trend toward warmer and wetter conditions over the 20th century (blue curves in Fig. 1D), supporting the central Pacific rainfall increase in response to anthropogenic forcing found in models. On shorter time scales, these time series display opposite signals, capturing the contrast between warm-wet and cold-dry regions related to the internal TPDV pattern (Fig. 1A). Recent advances in paleoclimate data assimilation have enabled the construction of gridded tropical Pacific SST fields extending through the past millennium (*19*) that match qualitatively well with the observed SST evolution over the instrumental period (Fig. 1D). These reconstructions, however, exhibit increasing uncertainty because fewer records become available back in time (gray shading in Fig. 1D).

Internal TPDV

The dominant internal TPDV SST signal can be characterized by the leading empirical orthogonal function and related principal component of 8- to 40-year variability of tropical Pacific SST (Fig. 2, A and B), which accounts for about half of the tropical Pacific SST variability in the 8- to 40-year time scale (contours in Fig. 1C). The related SST pattern throughout the entire Pacific basin can then be obtained through linear regression upon this principal component. This internal TPDV SST pattern (shading in Fig. 2A) strongly resembles the ENSO SST pattern in the tropics (Fig. 2E) but has a generally broader latitudinal extent (*20*, *21*). This pattern is also associated with a zonal seesaw in tropical Pacific mean sea level pressure, as described by the Southern Oscillation index (Fig. 2B), a measure of the difference in sea level pressure between Tahiti and Darwin, leading to the anticorrelation between this index and the SST-based internal TPDV index at decadal time scales (Fig. 2B). The internal TPDV SST pattern (Fig. 2A) is consistent with the patterns of variability associated with the Interdecadal Pacific Oscillation (*8*) over the Pacific basin and the Pacific Decadal Oscillation in the North Pacific (*22*), highlighting the important role of the tropical Pacific in forcing and synchronizing decadal variability in both hemispheres (*22*).

The simplest explanation for internal TPDV—the null hypothesis—is that it arises as a residual of largely independent ENSO events (*21*, *23*, *24*). We hence first establish the extent to which observed TPDV might result from decadal averages of ENSO events that are randomly distributed, without modification by independent decadal dynamics or decadal clustering through nonlinear interactions. In this view, the random

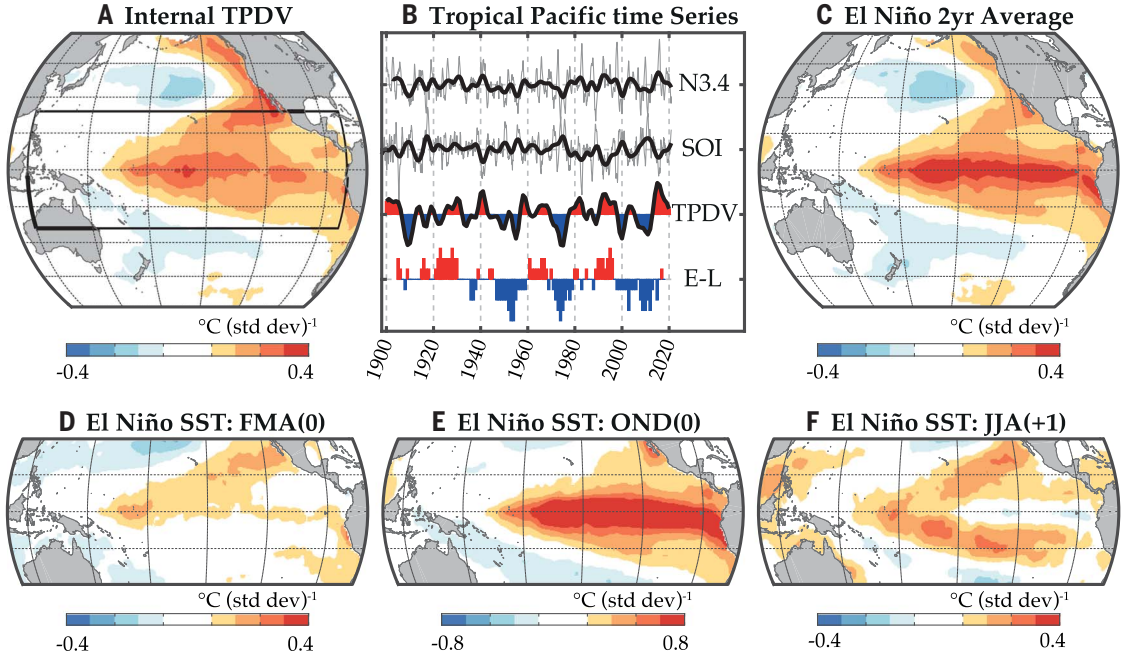

Fig. 2. Internal TPDV—the null hypothesis. (**A**) Pacific SST pattern associated with internal TPDV, obtained by regressing the 8- to 40-year band-pass filtered SST anomalies onto the internal TPDV index. The latter is obtained as the time series (or principal component) of the leading empirical orthogonal functions (EOF) of SST anomalies in the 8- to 40-year band, over the tropical Pacific (24°S to 24°N; 120°E to 80°W). (**B**) Time series of SST anomalies averaged in the Niño34 region (5°S to 5°N, 170°W to 120°W; N3.4), a commonly used SST ENSO index; the Southern Oscillation Index [SOI; (*18*)], a measure of the Walker circulation strength; the internal TPDV index; and the E-L index, defined as the number of El Niño years minus the number of La Niña years over 8-year running periods. ENSO events are identified using the December Niño3.4 index and an amplitude threshold of 1 standard deviation. Thick black lines in (B) indicate the 8- to 40-year band-pass filtered time series. (**C**) Average of ENSO-related SST anomalies over the year preceding the peak of an El Niño event (year 0) and the year after the El Niño event (year 1), defined by computing lagged regressions of SST onto the November-December-January averaged N3.4 index from lags of −11 months to +12 months, and averaging over all 24 resulting maps. (**D** to **F**) Individual SST maps from these monthly regressions, illustrating precursor anomalies during the February-March-April (FMA) (D) before the peak of an event, peak anomalies during October-November-December (OND) (E) of the ENSO event, and anomalies during the decay phase in June-July-August (JJA) (F) of the years after the peak of an ENSO event. The SST data are from HadISST (*96*) over the period 1900 to 2020. Filtering was performed using 5- and 53-point Hanning filter weights.

occurrence of decadal epochs with a larger number of El Niño (La Niña) events can be expected to result in an El Niño (La Niña)–like residual SST anomaly (*21*). The null hypothsis is supported by the good correspondence between the time series of the leading pattern of internal TPDV and the relative number of El Niño and La Niña events during partially overlapping 8-year periods (Fig. 2B). In addition, each ENSO event is not a static pattern but undergoes an evolution from a precursor phase (Fig. 2D), through a mature phase (Fig. 2E), to a decay phase (Fig. 2F), so that the average over this seasonal evolution across multiple events can result in a latitudinally broader pattern (Fig. 2C) very similar to the pattern in Fig. 2A (*24*).

This picture is further modified by ENSO asymmetries. For example, the strongest El Niño events are larger than the strongest La Niña events, La Niña events tend to last longer than El Niño events, and strong El Niño events tend to occur further east than strong La Niña events, affecting the details of TPDV (*25*). Differences in spatial patterns, with some events having greatest amplitude in the central or eastern tropical Pacific (*1*, *26*), may result in mean pattern differences during different decadal epochs (*25*), which may themselves occur purely by chance (*25*, *27*).

Whether decadal changes in the background state, even if randomly forced, feed back and modulate ENSO characteristics is a focus of current research (*28*). To go beyond the null hypothesis, therefore, we would need evidence that slow oceanic processes provide sources of decadal predictability beyond the ENSO time scale. For example, the ocean integration of ENSO-related surface fluxes may result in low-frequency SST variations with enhanced decadal predictability, as illustrated in a modeling context (*21*).

In addition, changes in the strength of the wind-driven upper-ocean overturning circulation, known as the subtropical-tropical cells (STCs), which connect the subtropical and equatorial regions, have been related to decadal variations of equatorial SSTs in both observations (*29*) and models (*30*, *31*). As schematically depicted in Fig. 3A, the STCs include subsurface equatorward flow, equatorial upwelling, and poleward flow in the surface Ekman layer, so that a strengthening (weakening) of the STCs results in enhanced (reduced) equatorial upwelling of cold subsurface waters, affecting equatorial SSTs. The adjustment of the STCs to changes in surface-wind forcing is accomplished through the propagation of oceanic Rossby waves (*30*) that travel to the western ocean boundary and then along the boundary to the equator as coastal-trapped waves, where they alter the depth of the equatorial thermocline and influence SST anomalies (Fig. 3A) (*32*, *33*). Because Rossby waves are more efficiently excited by wind anomalies with larger spatial scales and longer time scales, they can dynamically "filter" the wind forcing and contribute to an enhancement of low-frequency power (*34*).

Other modeling studies suggest that temperature anomalies subducted in the subtropics can reach the equatorial thermocline and influence equatorial SSTs (*35*), especially when they are density-compensated by associated salinity anomalies (so-called "spiciness" anomalies) and can then propagate toward the equator along mean density surfaces with minimal dissipation (*36*). Although the ability of spiciness anomalies to reach the equator from their source regions has been recently

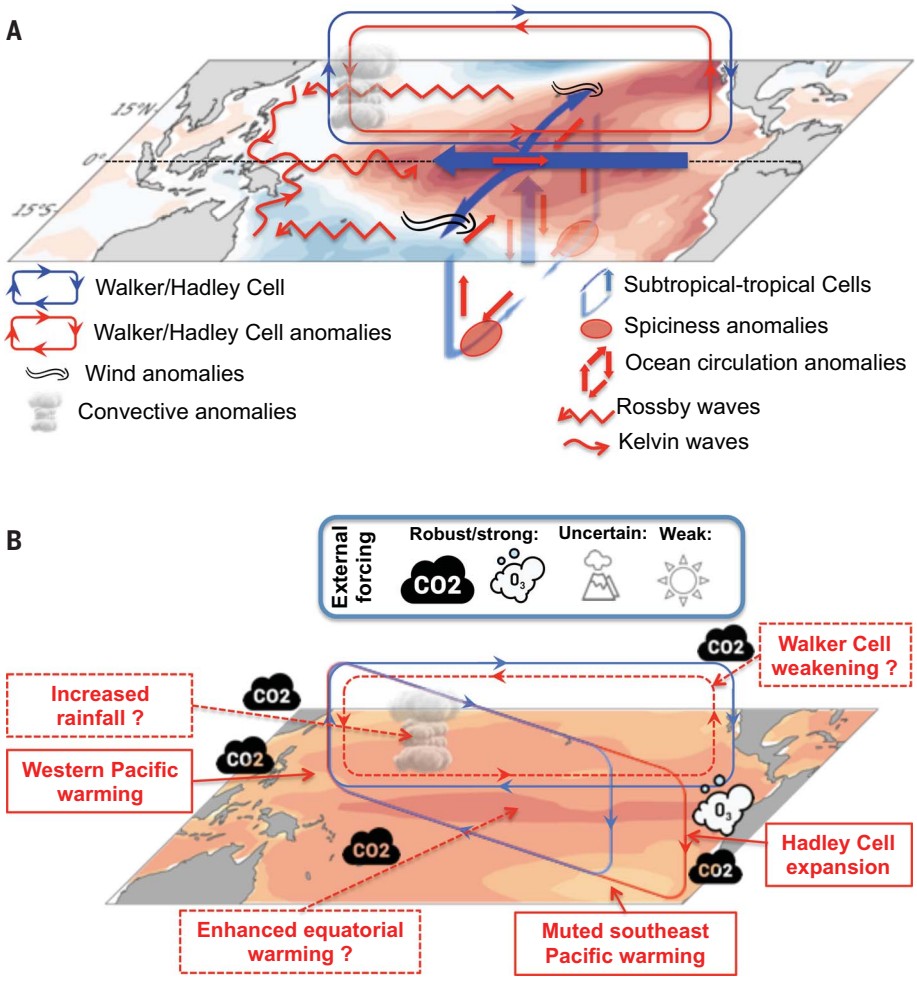

Fig. 3. Mechanisms of internal and external TPDV. (**A**) Schematic representation of the ocean processes associated with internal TPDV. The climatological upper-ocean overturning circulation (the STCs, transparent blue arrows) consists of a subtropical subduction component, equatorward subsurface transport, equatorial upwelling, and a poleward surface return flow driven by the equatorial easterly trade winds (large blue arrow), which are the surface components of the Walker circulation. A positive phase of internal TPDV with warm SST in the tropical Pacific (shading) is associated with a weaker Walker circulation, reduced equatorial winds, and weaker oceanic overturning circulation. Extra-equatorial wind anomalies may play an important role in driving the changes in the STCs, whose adjustment is accomplished through the westward propagation of oceanic Rossby waves. After reaching the western boundary, Rossby waves can continue along the boundary to the equator as coastal Kelvin waves and along the equator as equatorial Kelvin waves. The extra-equatorial wind anomalies may be purely stochastic or may arise from extratropical influences or as a response to equatorial SST anomalies (see text for details). (**B**) Schematic representation of projected changes associated with external TPDV. The map shows the late-21st century multimodel mean change in Coupled Model Intercomparison Project phase 6 (CMIP6) SST, which is dominated by increases in GHGs. High (low) confidence in these projected changes is indicated by solid (dashed) lines. Icons indicate the major external forcings involved in these changes. GHG increases and ozone changes induce a robust southward expansion of the Hadley cell in the Southern Hemisphere and reduced southern subtropical Pacific warming, in both model projections and observations. The prominent western Pacific warming and the central Pacific rainfall increase detected in models and observations can confidently be attributed to GHG increases. Although the projected weakening and enhanced tropical warming are evident in most CMIP6 models, confidence in these projections is low because of inconsistent signals in observations, model biases, and the complexity of the mechanisms involved. Volcanic eruptions and changes in solar insolation may also cause decadal variations in the tropical Pacific, though their amplitude is likely small.

demonstrated in a modeling context (*36*), their impact on equatorial SSTs in nature remains to be determined.

The above ocean processes occurring on decadal time scales are mostly wind-forced. In particular, modeling studies (*31*) indicate that subtropical winds play a key role in altering the strength of the STCs, but the origin of these anomalous winds is still unclear. Extratropical influences could be a source of subtropical wind variations. For example, internal atmospheric variability in the northern midlatitudes during winter can create subtropical SST and wind anomalies that persist through summer because of strong air-sea coupling (*37*), developing into a SST pattern that extends from the coast of California toward the central-western equatorial Pacific (Fig. 2D), known as the North Pacific Meridional Mode (*38*). Similarly, an anomalous SST pattern, known as the South Pacific Meridional Mode (*39*), can develop along the coast of South America (Fig. 2D). These meridional modes are considered ENSO precursors, but their associated winds could also provide anomalous forcing for the slow tropical oceanic processes described above (*40*). As ENSO precursors, they are also part of a seasonal progression from the extra-equatorial ENSO precursor stage, to ENSO development, to extratropical ENSO teleconnections that can act as a filter of decadal variance in the Pacific basin (*41*). Climate model sensitivity experiments, where the North and South Pacific Meridional Modes were alternatively suppressed (*42*), suggest a potentially more important influence of the South Pacific on internal TPDV, consistent with other model-based studies (*43*, *44*). SST anomalies in the Atlantic and Indian Oceans could also influence these tropical Pacific winds (*45*, *46*), as discussed below.

Finally, changes in subtropical-tropical winds may arise as a response to the equatorial SST anomalies themselves, as shown in some modeling studies (*32*, *47*). In this view, atmospheric teleconnections triggered by the tropical SST anomalies at decadal time scales alter the extra-equatorial atmospheric circulation and produce wind anomalies of the opposite sign that force a phase reversal of the decadal cycle. This view of internal TPDV as arising from low-frequency processes that are independent of ENSO, with important implications for decadal predictability, remains very challenging to demonstrate observationally, owing to the insufficient duration of the instrumental record in the presence of climate noise that may obscure the various deterministic links.

Representation of internal TPDV in climate models

In practice, evaluating internal TPDV simulated by climate models is challenging because (i) the instrumental record is relatively short (e.g., Fig. 1D), (ii) relatively few multicentury paleoclimate records exist for the core regions

of internal TPDV, (iii) internal TPDV in climate model simulations exhibits large changes from one century to the next (*48*), and (iv) the characteristics of internal TPDV vary markedly from model to model (Fig. 4).

As illustrated in Fig. 4, climate models still display major deficiencies in simulating key aspects of internal TPDV (*49*, *50*). For example, most models capture to first order the observed SST pattern, but the equatorial Pacific warming extends too far to the west [compare shading in Fig. 4, A and B; see also (*49*)], as do simulated ENSO SST patterns (*51*). Models also markedly underestimate sea level signals in the tropical western Pacific and extratropical central Pacific that are associated with internal TPDV (compare contours on Fig. 4, A and B). Similarly, the magnitude of simulated internal TPDV varies considerably from one model to another and is underestimated by most models not only in terms of SST (Fig. 4C) but also in terms of trade-wind strength (compare Fig. 4, A and B) and associated mean sea level pressure gradients in the tropical Pacific atmosphere (*4*, *52*). This underestimation partly arises because ENSO simulations in most models tend to be too quasi-biennial and not persistent enough (*53*), impeding the ability of models to generate decadal anomalies through the null hypothesis (*52*). As a consequence, although all models exhibit some link between ENSO decadal variability and internal TPDV, they strongly underestimate the strength of this relationship (Fig. 4D).

Sources of externally forced TPDV

As mentioned above, external radiative forcing from natural (e.g., volcanic eruptions and solar variability) and anthropogenic (e.g., GHGs, ozone, and sulfate aerosols) sources also contribute to TPDV. The resulting external TPDV is directly related to decadal variability in the forcing (e.g., intermittent volcanic eruptions, slowly increasing GHGs, varying anthropogenic aerosols emission), with possible contributions from the slow adjustment time scale of the ocean. In this section, we examine the expected tropical Pacific responses from both anthropogenic and natural external forcing, which are represented schematically in Fig. 3B.

GHGs such as carbon dioxide are the major source of anthropogenic climate warming and have been increasing steadily over past decades. Despite the spatially uniform nature of well-mixed GHGs, the warming of the ocean surface simulated by climate models exhibits substantial spatial variations (*54*). Most models project an enhanced warming in the equatorial Pacific (Fig. 3B), giving rise to tropical rainfall changes (*54*), altering global teleconnection patterns, increasing the frequency of extreme ENSO events (*55*), and regulating the magnitude of climate sensitivity (*56*). One study concluded that a GHG-forced enhancement of oceanic stratification leads to increasing Rossby wave speed, which decreases the amplitude and shortens the period of internal TPDV (*57*), whereas another study using a single model found that GHG enhanced the amplitude of internal decadal variability (*58*).

Unlike GHGs, anthropogenic tropospheric aerosols display large spatiotemporal variations because of localized emission sources and act to cool global surface temperature by reflecting sunlight. Models suggest that they induce SST and rainfall changes that are similar in pattern but opposite in sign to those of GHGs, especially in the tropical Pacific (*59*), hence weakening the GHG-induced warming.

Large volcanic eruptions can also contribute to external TPDV by injecting aerosols into the stratosphere. This cools the troposphere for a year or more (*2*) and the ocean for up to a decade—thereby temporarily reducing the rate of global thermosteric sea level rise (*60*). Although the impact of volcanic eruptions on global temperature is evident, their contribution to external TPDV is less clear (*61*, *62*). Volcanic eruptions have been suggested to (i) influence ENSO (*63*) and, by inference, TPDV and (ii) contribute to cooling the western Pacific warm pool on decadal scales (*64*). Models tend to simulate enhanced, long-term cooling in the eastern equatorial Pacific, but observations are still too sparse to adequately test these model results (*65*).

Confidence in the attribution of observed changes and future projections

Although GHG forcing generally dominates external TPDV at multidecadal and longer time scales, anthropogenic aerosols and volcanic eruptions may have substantially contributed to regional tropical SST variations over recent decades (*61*, *62*). Relatively small decadal changes in top-of-atmosphere solar irradiance presumably have a smaller influence than GHG, although the 11-year solar cycle, amplified by coupled atmosphere-ocean processes, has been proposed to modulate the Walker circulation on decadal time scales (*66*). Time scales involved in internal and external

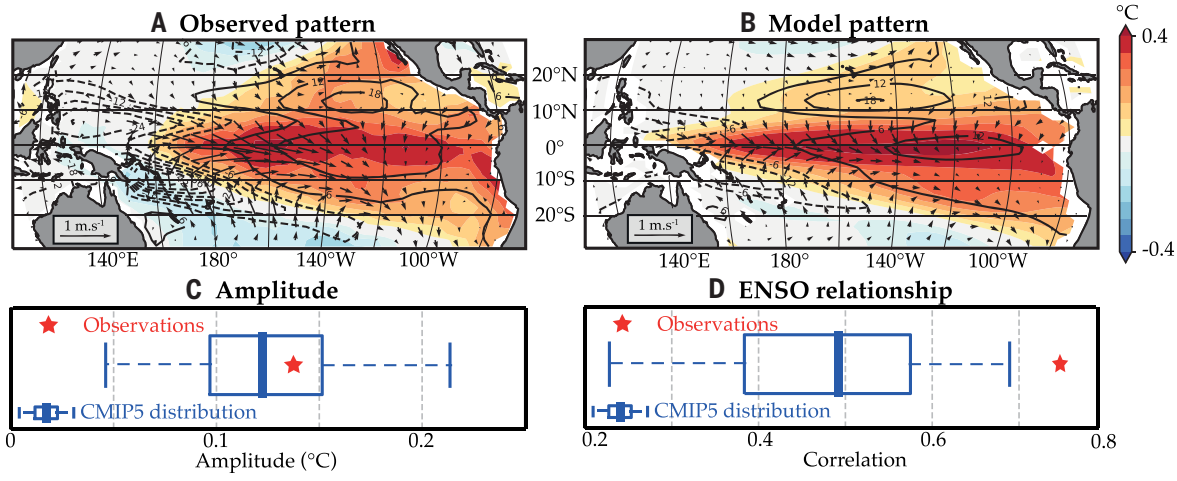

Fig. 4. Evaluation of internal TPDV in CMIP models. (**A** and **B**) Maps of the first EOF of 8- to 40-year band-pass filtered SST over the tropical Pacific (shading) and associated sea level (contours) and 2-m wind (vectors) variability for observations (*96*, *98*, *99*) (A) and a multimodel mean of (*10*) (B). (**C** and **D**) Box plot showing median, interquartile range, maximum, and minimum of CMIP6 historical simulations for the standard deviation of the TPDV index (C) and the correlation coefficients between E-L and the internal TPDV index (D). E-L is a measure of the extent to which El Niño dominates each 8-year period and is defined as n(EN) − n(LN), where n(EN) is the number of El Niño years and n(LN) is the number of La Niña years in 8-year blocks. ENSO events are defined using a threshold of 1 standard deviation of Nino3.4 SST. The TPDV index is defined here as the first principal component of the 8- to 40-year band-pass filtered SST EOF analysis. Observations are shown as a red star.

TPDV overlap, which makes them difficult to distinguish from one another, especially when considering the relatively short climate record and potential errors in models. As a result, there are varying degrees of confidence in the attribution of some of the observed trends to either internal or external forcing. In the next section, we discuss key aspects of future model projections in the tropical Pacific, comparing them with the observational record.

Western Pacific warming

The western Pacific has exhibited a prominent warming trend since the 1950s (Figs. 1D and 5A), which dominates the evolution of SST in this region (Fig. 1B). This warming trend is accurately captured by historical simulations (compare Fig. 5, A and B) and clearly stands out against the weak background natural variability in this region (Fig. 5C), reflecting the fact that the signal-to-noise ratio for this projected warming is among the highest in the world (*12*). Coral-based SST estimates indicate that such a warming period is likely unprecedented in the western Pacific region throughout the past 1250 years (*67*). The warming trend for air temperatures over land in west Pacific island countries is so large that every year since the early 1990s has been warmer than all the years before 1970 (*68*). The resulting increase of the western Pacific warm-pool size has confidently been attributed to GHG forcing arising from human activity (*68*, *69*), although remote influence from the natural multidecadal climate variability in the Atlantic (*70*) and major volcanic eruptions (*64*) may also have modulated the SST warming rate there.

Hadley cell

Although recent observational datasets significantly differ before the 1950s, they consistently report a southward expansion of the southern edge of the Southern Hemisphere Hadley cell since 1979 [Fig. 5D; (*71*)]. Although internal climate variability also contributed, this widening over the past 40 years can confidently be attributed to the combined effect of ozone depletion and rising GHGs [Figs. 3B and 5D; (*71*)]. The mechanism behind this widening is still subject to debate but likely reflects how subtropical atmospheric baroclinic eddies respond to tropospheric (GHGs) and stratospheric (ozone) changes in the atmospheric background state (*71*). This southward expansion is associated with a lower rate of warming (Fig. 5, A and B) and ocean acidification (*54*, *72*) in the southeastern tropical Pacific than in the rest of the tropics, probably driven by an intensification of the southeastern Pacific trade winds, which strengthen the Peru-Chile upwelling system near the coast, increase heat loss through air-sea fluxes, and modulate the oceanic mixed

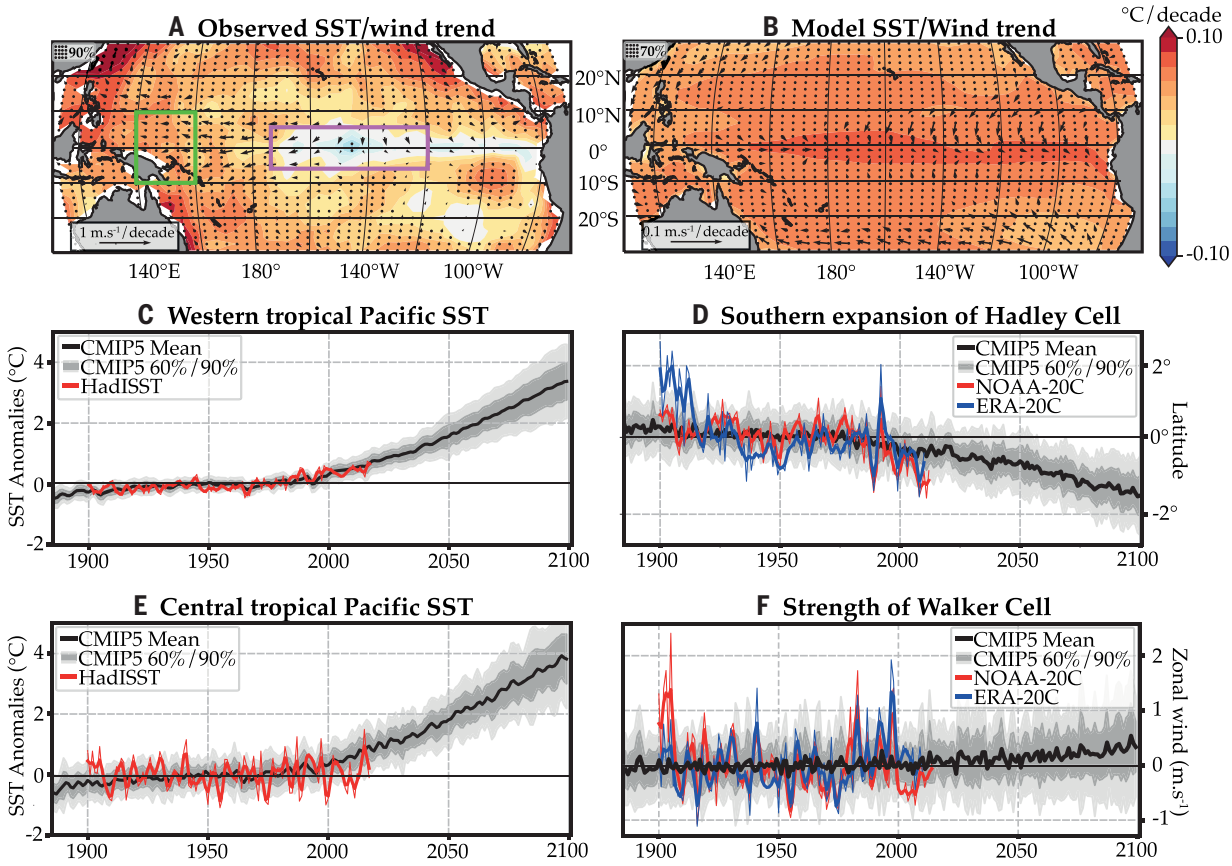

Fig. 5. Detection and attribution of long-term trends in the tropical Pacific. (**A** and **B**) Observed (*96*, *98*, *99*) (A) and multimodel mean (*10*) (B) maps of 1900–2009 linear trends of SST (shading) and surface winds (vectors) over the tropical Pacific. (**C** to **F**) Annual time series for CMIP6 historical simulations (gray) and observations (colored) of the SST averaged over the western tropical Pacific (10°N to 10°S; 120°E to 150°E) (C) and the Niño34 region (5°N to 5°S; 170°W to 120°W) (E), the latitude of the Southern Hemisphere Hadley cell's poleward edge (D), and the strength of equatorial zonal (east-west) winds (F). The latitude of the Southern Hemisphere Hadley cell's poleward edge is defined as the latitude where zonal mean precipitation-evaporation is zero, while the strength of equatorial zonal (east-west) winds is diagnosed from the 10-m zonal wind anomalies in the Niño3.4 region (positive values indicate a weakening Walker circulation). CMIP6 results: Ensemble mean (black lines) and 60% (dark blue shading) and 90% (light blue shading) confidence intervals using a t-distribution. Reanalysis: NOAA 20th Century Reanalysis (NOAA-20C) (red) (*99*) and the ECMWF 20th Century Reanalysis (ERA-20C) (blue) (*100*); red lines indicate annual anomalies (thin lines); and 8-year running averages (thick lines) are shown. SST data: HadISST (*96*). Note that the spread of model simulations is larger in the Niño3.4 region than in the western Pacific. The Hadley cell is calculated over all longitudes, not just the Pacific.

layer offshore (68). Models also project a widening of the Northern Hemisphere Hadley cell that, as of now, is not yet detectable in observations owing to a larger influence of internal climate variability (71, 73).

The Walker circulation and equatorial SST gradients

As illustrated in Fig. 5, B, E, and F, most state-of-the-art models project a weakening of the equatorial trade winds and Walker circulation and a faster warming rate at the equator, in particular in the eastern equatorial Pacific (55). In agreement with instrumental observations and historical simulations (51, 74), central tropical Pacific corals also point to a wet trend over the 20th century (Fig. 1D), accompanied by even wetter periods during positive phases of the Interdecadal Pacific Oscillation (18). A leading explanation for the Walker circulation weakening is that rainfall increases less in models than predicted by the Clausius-Clapeyron relation, implying increased atmospheric stability and a reduced mass-flux between the boundary layer and free atmosphere, resulting in a weakened Walker circulation (75). The enhanced equatorial eastern Pacific warming has been explained by a feedback loop between the weaker evaporative cooling in the cold tongue (54) and reduced trade winds, and a limitation of the SST increase by cloud feedbacks over the West Pacific (55). Recent studies also suggest that the subtropical anthropogenic warming also contributes to the enhanced equatorial warming by slowly making its way to the equatorial thermocline through the oceanic STCs (76, 77). There is, however, no consensus to date on the dominant mechanism responsible for the projected equatorial Pacific SST gradient changes.

A key uncertainty of external TPDV is that simulated changes do not match recent observed historical trends over, for example, 1981 to 2012 (4, 52), which are characterized by a marked strengthening of the Walker circulation over this period. Such signals are typical of internal TPDV (Fig. 4, A and B). Indeed, recent studies attribute a large part of this recent observed evolution in the central equatorial Pacific to internal TPDV (4, 52, 78), which is a strong contributor to SST variations in this region (Fig. 1C). This is illustrated by the relatively large model ensemble spread displayed in Fig. 5, E and F, which largely encompasses the observed SST and surface wind evolution.

Conversely, many recent studies suggest plausible mechanisms by which external forcings might also have contributed to the recent strengthening. For example, model results indicate that the reduction in tropospheric sulfate aerosol emissions from North America and Europe and the concurrent increase in China—perhaps augmented by changes driven by volcanic eruptions (62, 79)—might have contributed to the recent tropical Pacific cooling (61). Other modeling studies suggest that the observed faster warming in the Indian and/or Atlantic Oceans relative to the Pacific Ocean is conducive to enhanced trades in the Pacific and reinforced the recent tropical Pacific cooling (46). Increasing GHGs likely contributed to this observed Indian-Pacific differential warming, but their contribution to the enhanced Atlantic warming is unclear (80). Finally, some models reproduce the observed Walker circulation strengthening and equatorial cooling (81), with a plausible mechanism related to the poleward export of the added equatorial Pacific heat by the sustained meridional divergence of the near-equatorial upper-ocean currents (82, 83). Model-based studies further suggest that the fast equatorial cooling related to this oceanic thermostat mechanism will be followed by a slower transition to an enhanced equatorial warming and Walker circulation weakening, in response to subtropical warm anomalies advected into the equatorial thermocline by the STCs (76, 77).

It is thus unclear from current literature whether the recent observed Walker circulation and cold-tongue strengthening is a response to external forcing that is only reproduced by a few models or whether it simply arises from internal variability hiding a subtle opposite secular trend (78). This results in a rather low confidence in the projected weakening of the Walker circulation and related enhanced equatorial eastern Pacific warming in climate models. Several studies indeed argue that the enhanced equatorial warming in most climate projections may arise from common present-day climate model biases within the tropical Pacific (84) or from an underestimation of interbasin interactions (45, 46, 84). Confidence in these projections is further reduced by the large uncertainties on the impact of aerosols on radiation, cloud microphysics, and SST (85). These caveats imply that it is not possible as of now to conclude with confidence whether GHG forcing has weakened, has strengthened, or has had no effect on the Walker circulation and equatorial upwelling.

Changes in ENSO

Improving the reliability of these projections is key, partly because projected changes in the equatorial zonal SST gradient strongly influence ENSO in climate models (55). The projected warming pattern in the equatorial Pacific in most climate models indeed increases ENSO-driven and decadal precipitation anomalies in part of the tropical Pacific (51, 55, 74) and is tied to an increase in the amplitude of ENSO anomalies (55). Recent paleoclimatic evidence suggests that the increase in ENSO variability since the 1950s stands out in the context of the past millennia (86), lending support to the intermodel agreement on increased ENSO-driven precipitation variability under greenhouse warming. These findings have important implications, given the large societal impacts of projected changes in ENSO and the fact that any increase in ENSO-driven precipitation variability (51) or the frequency of extreme ENSO states (55) may energize internal TPDV through the various forms of our null hypothesis (21, 24, 25).

Outlook

Predicting the climate of the tropical Pacific over the next decade and beyond—including precipitation, temperature, sea level, and biogeochemistry—would have far-reaching societal and environmental benefits. However, because of the partially chaotic nature of the climate system, decadal predictions can, at best, provide an outlook of annual to multiyear average conditions or risks, rather than a more detailed picture of daily or seasonal conditions (2). A decadal prediction would be typically expressed in terms of probabilities, such as the probability that temperature in the tropical Pacific averaged over the next 5 years will exceed the temperature in the tropical Pacific averaged over the past 30 years. Although the changes in average conditions may be small, they can produce marked differences in the probability of extremes (12).

Experimental prediction systems have been developed (2, 14) to exploit any predictability arising from the mechanisms discussed in the previous sections. Results from an ensemble prediction system suggest that initialization with observations in much of the tropical Pacific tends to contribute toward predictive skill for surface temperature, for forecast lead times only up to about 2 years (Fig. 6A), and is mostly associated with predictability arising from ENSO (87), though another study concluded that transbasin climate variability connected with TPDV can be predicted up to 3 years in advance (46). It might also be that climate models underestimate the degree of skill that actually exists in the real world (88). At longer lead times, skill arises mainly from external forcing (2, 89) (Fig. 6A).

Although predictive skill of decadal average SST is found in most of the tropical Pacific (15, 87) (Fig. 6B), it is not evident everywhere. In particular, there is limited skill in the central tropical Pacific north of the equator, extending to the northeast Pacific (Fig. 6B). This is an important region because SST variability there can affect climate in many parts of the world. This low skill may be because the intrinsic predictability of internal variability beyond 2 years is genuinely low there and any predictable forced response is weak compared with unpredictable internal variability. Alternatively, the combined impact of internal variability and the externally forced signal may be predictable, but the models might miss

or misrepresent key mechanisms underpinning the predictability. If this is the case, then the impact of TPDV on ENSO behavior might also be underestimated to date.

An important advancement identified in this review is that skill in decadal predictions of SST in the western Pacific is apparent in the past two generations of dynamical decadal prediction systems (*2*) (Fig. 6B). Although it is likely that this primarily arises from anthropogenic warming, climate models also simulate substantial externally forced decadal variability in this region about the long-term warming trend (Fig. 5C). This suggests that other types of external forcing have also contributed to TPDV in western Pacific SSTs. Whether this enhances predictability in western Pacific SSTs or not is still unclear.

There are indications that in the tropical Pacific, multiyear variability in some biogeochemical quantities important for fisheries and the global carbon budget such as net primary production and carbon dioxide uptake can be predicted with greater skill than SST (*90*, *91*). This may be because the biogeochemical quantities are more influenced by subsurface and spatially integrated quantities, which tend to exhibit greater predictability than SST (*21*). Limited evidence also suggests that there may be some skill in predicting atmospheric sea level pressure and sea surface height (*92*); changes in the phase of the Interdecadal Pacific Oscillation [e.g., (*93*, *94*]; related precipitation averaged over the Asian-Australian monsoon, Australia more broadly, and western North America (*95*); and soil moisture—with implications for drought and wildfire—over parts of the southwestern United States (*6*).

Our review of TPDV predictability finds that although responses to anthropogenic GHG increases offer predictability in some variables (e.g., Figs. 5C and 6, A and B), confidence in the modeled response in the tropical Pacific is generally low; predictability from tropospheric aerosols is still debated; volcanic eruptions likely provide predictability immediately after the eruption has occurred (*63*); changes in anthropogenic aerosols (e.g., due to industrial growth and pollution aerosols) provide longer–time scale forcing; and TPDV arising from solar forcing likely exists but is small in models compared with other sources of external forcing and unlikely to be a substantial source of predictability.

The way forward

This review has highlighted some important advances in our understanding of the tropical Pacific climate variability and change at decadal and longer time scales. It has also highlighted the complexity of the interactions between variations that occur naturally and those that are forced by external factors of both natural and anthropogenic origin and the knowledge gaps and uncertainties associated with both components and their interactions. Although several plausible mechanisms for both internal and externally forced TPDV have been proposed, their relative importance and relevance to predictability need to be further clarified. Specific open questions include the following:

1. How important are oceanic processes involving the STCs in driving predictable decadal climate variations? Do the mechanisms involving STC variability and the associated wind forcing arise independently of ENSO? How large is the predictability associated with these oceanic processes?

2. How robust are climate model projections in the tropical Pacific, and what are the dominant processes driving these changes? In particular, how will the Walker circulation, equatorial SST, and internal variability respond to future GHG increases?

3. Why do forecast systems appear to offer predictive skill in the western and southern tropical Pacific but not in the northeastern tropical Pacific?

Improvements in the quality, quantity, and length of observational records available for characterizing decadal variability are critical to address these questions and to initialize and verify decadal prediction systems. This will require sustaining and enhancing the ocean and climate observing systems, data rescue efforts to recover historical observations from data-sparse regions, and the development of new monthly to annually resolved paleoclimate records from TPDV centers of action, with a focus on obtaining multiple records in those regions to enhance signal-to-noise ratios. Continued advances in paleoclimate data assimilation (*19*) will also be critical for the integration of paleoclimate and instrumental observations with models to obtain more complete and reliable fields.

Although substantial model improvements have been made in recent decades for some features of the climate system (*10*), models are still limited in their ability to accurately represent observed TPDV, and there are large model-to-model differences in the magnitude of simulated TPDV. As noted in the introduction, there is evidence suggesting that there may be a link between these differences and model-to-model differences in global climate sensitivity. Improving the simulation of TPDV might therefore yield a narrower range in climate sensitivities and greater clarity about our climatic future.

Despite their shortcomings, climate models are essential tools for advancing our ability to understand and predict future change in the tropical Pacific. The underlying causes of the shortcomings are still elusive, and dedicated efforts using innovative approaches are required to identify the major sources of errors in both local and remote feedbacks. Enhanced efforts on the specific role of the STCs in driving TPDV in models may facilitate improved understanding of the mechanisms involving variability of the STCs and their associated wind forcing. In the longer term, improving climate models will be essential for achieving more realistic simulations, as well as more

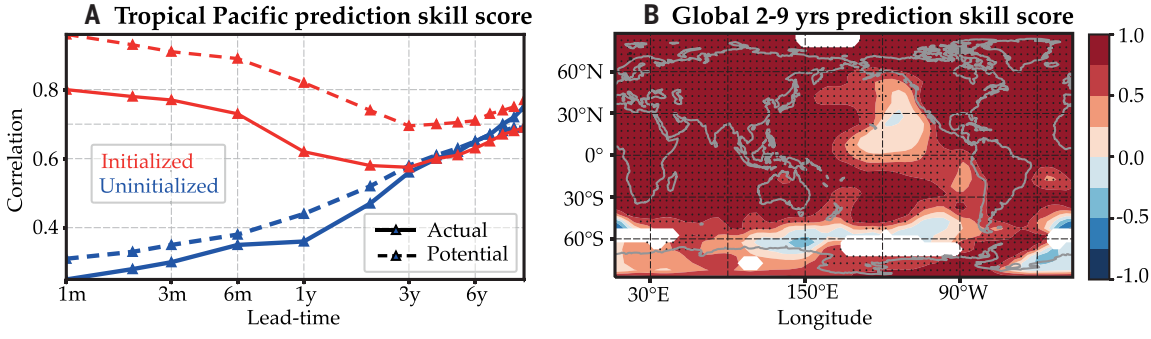

Fig. 6. Predicting TPDV. (**A**) Actual (solid lines) and potential (dashed lines) correlation skill for the surface air temperature averaged over the tropical Pacific as a function of lead time, for initialized forecasts (red) and for uninitialized simulations (blue), estimated using methods described previously (*15*). The difference between the initialized and uninitialized simulations is an indication of the potential for forecast improvement (*15*). (**B**) Correlation skill score using 8-year running mean observations of near-surface air temperature and forecast years 2 to 9 from initialized multimodel decadal predictions. Skill is measured using the mean of 71 ensemble members from seven modeling systems (*89*). Darker red indicates higher estimated skill. Hindcasts (*2*) starting every year from 1960 to 2005, with observations described previously (*89*), are shown. Stippling indicates that the value is outside of the 95% confidence interval.

reliable predictions and projections, of TPDV. Advances are expected from improvements in the representation of subgridscale processes, data assimilation into forecast systems, and computing technology that enables higher spatial resolution, less reliance on parameterizations, longer model runs, and larger ensemble sizes.

REFERENCES AND NOTES

1. A. Timmermann *et al.*, El Niño-Southern Oscillation complexity. *Nature* **559**, 535–545 (2018). doi: 10.1038/s41586-018-0252-6; pmid: 30046070
2. B. Kirtman *et al.*, "Near-term climate change: Projections and predictability" in *Climate Change 2013: The Physical Science Basis. Contribution of Working Group I to the Fifth Assessment Report of the Intergovernmental Panel on Climate Change*, T. F. Stocker, D. Qin, G.-K. Plattner, M. Tignor, S. K. Allen, J. Boschung, A. Nauels, Y. Xia, V. Bex, P. M. Midgley, Eds. (Cambridge Univ. Press, 2013), pp. 953–1028.
3. Y. Kosaka, S. P. Xie, Recent global-warming hiatus tied to equatorial Pacific surface cooling. *Nature* **501**, 403–407 (2013). doi: 10.1038/nature12534; pmid: 23995690
4. M. H. England *et al.*, Recent intensification of wind-driven circulation in the Pacific and the ongoing warming hiatus. *Nat. Clim. Chang.* **4**, 222–227 (2014). doi: 10.1038/nclimate2106
5. X. Zhang, J. A. Church, Sea level trends, interannual and decadal variability in the Pacific Ocean. *Geophys. Res. Lett.* **39**, L21701 (2012). doi: 10.1029/2012GL053240
6. Y. Chikamoto, A. Timmermann, M. J. Widlansky, M. A. Balmaseda, L. Stott, Multi-year predictability of climate, drought, and wildfire in southwestern North America. *Sci. Rep.* **7**, 6568 (2017). doi: 10.1038/s41598-017-06869-7; pmid: 28747719
7. G. A. Meehl, J. M. Arblaster, C. M. Bitz, C. T. Y. Chung, H. Teng, Antarctic sea-ice expansion between 2000 and 2014 driven by tropical Pacific decadal climate variability. *Nat. Geosci.* **9**, 590–595 (2016). doi: 10.1038/ngeo2751
8. S. Power, T. Casey, C. Folland, A. Colman, V. Mehta, Inter-decadal modulation of the impact of ENSO on Australia. *Clim. Dyn.* **15**, 319–324 (1999). doi: 10.1007/s003820050284
9. R. Colman, S. B. Power, What can decadal variability tell us about climate feedbacks and sensitivity? *Clim. Dyn.* **51**, 3815–3828 (2018). doi: 10.1007/s00382-018-4113-7
10. Intergovernmental Panel on Climate Change (IPCC), *Climate Change 2013: The Physical Science Basis. Contribution of Working Group I to the Fifth Assessment Report of the Intergovernmental Panel on Climate Change*, T. F. Stocker *et al.*, Eds. (Cambridge Univ. Press, 2013).
11. L. Wang, G. Huang, W. Chen, W. Zhou, W. Wang, Wet-to-dry shift over Southwest China in 1994 tied to the warming of tropical warm pool. *Clim. Dyn.* **51**, 3111–3123 (2018). doi: 10.1007/s00382-018-4068-8
12. S. B. Power, F. P. D. Delage, Setting and smashing extreme temperature records over the coming century. *Nat. Clim. Chang.* **9**, 529–534 (2019). doi: 10.1038/s41558-019-0498-5
13. J. E. Johnson *et al.*, in *Climate Change and Impacts in the Pacific*, L. Kumar, Ed. (Springer Climate Series, Springer, 2020), pp. 359–402.
14. Y. Kushnir *et al.*, Towards operational predictions of the near-term climate. *Nat. Clim. Chang.* **9**, 94–101 (2019). doi: 10.1038/s41558-018-0359-7
15. G. J. Boer, G. J. Kharin, W. J. Merryfield, Differences in potential and actual skill in a decadal prediction experiment. *Clim. Dyn.* **52**, 6619–6631 (2019). doi: 10.1007/s00382-018-4533-4
16. J. E. Tierney *et al.*, Tropical sea surface temperatures for the past four centuries reconstructed from coral archives. *Paleoceanography* **30**, 226–252 (2015). doi: 10.1002/2014PA002717
17. E. P. Dassié, A. Hasson, M. Khodri, N. Lebas, B. K. Linsley, Spatiotemporal Variability of the South Pacific Convergence Zone Fresh Pool Eastern Front from Coral-Derived Surface Salinity Data. *J. Clim.* **31**, 3265–3288 (2017). doi: 10.1175/JCLI-D-17-0071.1
18. S. C. Sanchez *et al.*, A Continuous Record of Central Tropical Pacific Climate Since the Midnineteenth Century Reconstructed From Fanning and Palmyra Island Corals: A Case Study in Coral Data Reanalysis. *Paleoceanogr. Paleoclimatol.* **35**, 1–15 (2020). doi: 10.1029/2020PA003848
19. R. Tardif *et al.*, Last Millennium Reanalysis with an expanded proxy database and seasonal proxy modeling. *Clim. Past* **15**, 1251–1273 (2019). doi: 10.5194/cp-15-1251-2019
20. Y. Zhang, J. M. Wallace, D. S. Battisti, ENSO-like interdecadal variability: 1900-93. *J. Clim.* **10**, 1004–1020 (1997). doi: 10.1175/1520-0442(1997)010<1004:ELIV>2.0.CO;2
21. S. Power, R. Colman, Multi-year predictability in a coupled general circulation model. *Clim. Dyn.* **26**, 247–272 (2006). doi: 10.1007/s00382-005-0055-y
22. M. Newman *et al.*, The Pacific decadal oscillation, revisited. *J. Clim.* **29**, 4399–4427 (2016). doi: 10.1175/JCLI-D-15-0508.1
23. T. R. Ault, C. Deser, M. Newman, J. Emile-Geay, Characterizing decadal to centennial variability in the equatorial Pacific during the last millennium. *Geophys. Res. Lett.* **40**, 3450–3456 (2013). doi: 10.1002/grl.50647
24. D. J. Vimont, The Contribution of the Interannual ENSO Cycle to the Spatial Pattern of Decadal ENSO-Like Variability. *J. Clim.* **18**, 2080–2092 (2005). doi: 10.1175/JCLI3365.1
25. G. Il Kim, J. S. Kug, Tropical pacific decadal variability induced by nonlinear rectification of El Niño–Southern Oscillation. *J. Clim.* **33**, 7289–7302 (2020). doi: 10.1175/JCLI-D-19-0123.1
26. A. Capotondi, A. T. Wittenberg, J. Kug, K. Takahashi, M. J. McPhaden, in *El Niño Southern Oscillation in a Changing Climate*, M. J. McPhaden, A. Santoso, W. Cai, Eds. (Wiley, 2020), pp. 65–86.
27. M. Newman, S.-I. Shin, M. A. Alexander, Natural variation in ENSO flavors. *Geophys. Res. Lett.* **38**, n/a (2011). doi: 10.1029/2011GL047658
28. T. Sun, Y. M. Okumura, Impact of ENSO-Like Tropical Pacific Decadal Variability on the Relative Frequency of El Niño and La Niña Events. *Geophys. Res. Lett.* **47**, 1–10 (2020). doi: 10.1029/2019GL085832
29. M. J. McPhaden, D. Zhang, Slowdown of the meridional overturning circulation in the upper Pacific Ocean. *Nature* **415**, 603–608 (2002). doi: 10.1038/415603a; pmid: 11832936
30. A. Capotondi, M. A. Alexander, C. Deser, M. J. McPhaden, Anatomy and Decadal Evolution of the Pacific Subtropical–Tropical Cells (STCs). *J. Clim.* **18**, 3739–3758 (2005). doi: 10.1175/JCLI3496.1
31. G. Graffino, R. Farneti, F. Kucharski, F. Molteni, The effect of wind stress anomalies and location in driving Pacific subtropical cells and tropical climate. *J. Clim.* **32**, 1641–1660 (2019). doi: 10.1175/JCLI-D-18-0071.1
32. G. A. Meehl, A. Hu, Megadroughts in the Indian Monsoon Region and Southwest North America and a Mechanism for Associated Multidecadal Pacific Sea Surface Temperature Anomalies. *J. Clim.* **19**, 1605–1623 (2006). doi: 10.1175/JCLI3675.1
33. A. Capotondi, M. A. Alexander, Rossby waves in the tropical North Pacific and their role in decadal thermocline variability. *J. Phys. Oceanogr.* **31**, 3496–3515 (2001). doi: 10.1175/1520-0485(2002)031<3496:RWITTN>2.0.CO;2
34. A. Capotondi, M. A. Alexander, C. Deser, Why Are There Rossby Wave Maxima in the Pacific at 10°S and 13°N? *J. Phys. Oceanogr.* **33**, 1549–1563 (2003). doi: 10.1175/2407.1
35. J. Luo *et al.*, South Pacific origin of the decadal ENSO-like variation as simulated by a coupled GCM. *Geophys. Res. Lett.* **30**, 4–7 (2003).
36. M. Zeller, S. McGregor, E. van Sebille, A. Capotondi, P. Spence, Subtropical-tropical pathways of spiciness anomalies and their impact on equatorial Pacific temperature. *Clim. Dyn.* **56**, 1131–1144 (2020). doi: 10.1007/s00382-020-05524-8
37. D. J. Vimont, D. S. Battisti, A. C. Hirst, Footprinting: A seasonal connection between the tropics and mid-latitudes. *Geophys. Res. Lett.* **28**, 3923–3926 (2001). doi: 10.1029/2001GL013435
38. J. C. H. Chiang, D. J. Vimont, Analogous Pacific and Atlantic Meridional Modes of Tropical Atmosphere–Ocean Variability. *J. Clim.* **17**, 4143–4158 (2004). doi: 10.1175/JCLI4953.1
39. H. Zhang, A. Clement, P. Di Nezio, The South Pacific meridional mode: A mechanism for ENSO-like variability. *J. Clim.* **27**, 769–783 (2014). doi: 10.1175/JCLI-D-13-00082.1
40. E. Di Lorenzo *et al.*, ENSO and meridional modes: A null hypothesis for Pacific climate variability. *Geophys. Res. Lett.* **42**, 9440–9448 (2015). doi: 10.1002/2015GL066281
41. Y. Zhao, E. Di Lorenzo, The impacts of Extra-tropical ENSO Precursors on Tropical Pacific Decadal-scale Variability. *Sci. Rep.* **10**, 3031 (2020). doi: 10.1038/s41598-020-59253-3; pmid: 32080206
42. G. Liguori, E. Di Lorenzo, Separating the North and South Pacific Meridional Modes Contributions to ENSO and Tropical Decadal Variability. *Geophys. Res. Lett.* **46**, 906–915 (2019). doi: 10.1029/2018GL080320
43. Y. M. Okumura, Origins of tropical pacific decadal variability: Role of stochastic atmospheric forcing from the South Pacific. *J. Clim.* **26**, 9791–9796 (2013). doi: 10.1175/JCLI-D-13-00448.1
44. C. T. Y. Chung, S. B. Power, A. Sullivan, F. Delage, The role of the South Pacific in modulating Tropical Pacific variability. *Sci. Rep.* **9**, 18311 (2019). doi: 10.1038/s41598-019-52805-2; pmid: 31797940
45. S. McGregor, M. F. Stuecker, J. B. Kajtar, M. H. England, M. Collins, Model tropical Atlantic biases underpin diminished Pacific decadal variability. *Nat. Clim. Chang.* **8**, 493–498 (2018). doi: 10.1038/s41558-018-0163-4
46. W. Cai *et al.*, Pantropical climate interactions. *Science* **363**, eaav4236 (2019). doi: 10.1126/science.aav4236; pmid: 30819937
47. R. Farneti, F. Molteni, F. Kucharski, Pacific interdecadal variability driven by tropical-extratropical interactions. *Clim. Dyn.* **42**, 3337–3355 (2014). doi: 10.1007/s00382-013-1906-6
48. Y. Peng, C. Shen, H. Cheng, Y. Xu, Simulation of the Interdecadal Pacific Oscillation and its impacts on the climate over eastern China during the last millennium. *J. Geophys. Res. Atmos.* **120**, 7573–7585 (2015). doi: 10.1002/2015JD023104
49. K. Lyu, X. Zhang, J. A. Church, J. Hu, Evaluation of the interdecadal variability of sea surface temperature and sea level in the Pacific in CMIP3 and CMIP5 models. *Int. J. Climatol.* **36**, 3723–3740 (2016). doi: 10.1002/joc.4587
50. B. J. Henley *et al.*, Spatial and temporal agreement in climate model simulations of the Interdecadal Pacific Oscillation. *Environ. Res. Lett.* **12**, 044011 (2017). doi: 10.1088/1748-9326/aa5cc8
51. S. Power, F. Delage, C. Chung, G. Kociuba, K. Keay, Robust twenty-first-century projections of El Niño and related precipitation variability. *Nature* **502**, 541–545 (2013). doi: 10.1038/nature12580; pmid: 24121439
52. G. Kociuba, S. B. Power, Inability of CMIP5 models to simulate recent strengthening of the walker circulation: Implications for projections. *J. Clim.* **28**, 20–35 (2015). doi: 10.1175/JCLI-D-13-00752.1
53. H. Bellenger, E. Guilyardi, J. Leloup, M. Lengaigne, J. Vialard, ENSO representation in climate models : From CMIP3 to CMIP5. *Clim. Dyn.* **42**, 1999–2018 (2014). doi: 10.1007/s00382-013-1783-z
54. S.-P. Xie *et al.*, Global Warming Pattern Formation: Sea Surface Temperature and Rainfall. *J. Clim.* **23**, 966–986 (2010). doi: 10.1175/2009JCLI3329.1
55. W. Cai, A. Santoso, G. Wang, L. Wu, M. Collins, M. Lengaigne, S. Power, A. Timmermann, in *El Niño Southern Oscillation in a Changing Climate*, M. J. McPhaden, A. Santoso, W. Cai, Eds. (Wiley, 2020), pp. 289–307.doi: 10.1002/9781119548164.ch13
56. T. Andrews, J. M. Gregory, M. J. Webb, The dependence of radiative forcing and feedback on evolving patterns of surface temperature change in climate models. *J. Clim.* **28**, 1630–1648 (2015). doi: 10.1175/JCLI-D-14-00545.1
57. G. Liguori, E. Di Lorenzo, Meridional Modes and Increasing Pacific Decadal Variability Under Anthropogenic Forcing. *Geophys. Res. Lett.* **45**, 983–991 (2018). doi: 10.1002/2017GL076548
58. S. Li *et al.*, The Pacific Decadal Oscillation less predictable under greenhouse warming. *Nat. Clim. Chang.* **10**, 30–34 (2020). doi: 10.1038/s41558-019-0663-x
59. S.-P. Xie, B. Lu, B. Xiang, Similar spatial patterns of climate responses to aerosol and greenhouse gas changes. *Nat. Geosci.* **6**, 828–832 (2013). doi: 10.1038/ngeo1931
60. M. A. Balmaseda, K. E. Trenberth, E. Källén, Distinctive climate signals in reanalysis of global ocean heat content. *Geophys. Res. Lett.* **40**, 1754–1759 (2013). doi: 10.1002/grl.50382
61. D. M. Smith *et al.*, Role of volcanic and anthropogenic aerosols in the recent global surface warming slowdown. *Nat. Clim. Chang.* **6**, 936–940 (2016). doi: 10.1038/nclimate3058
62. W. Hua, A. Dai, M. Qin, Contributions of Internal Variability and External Forcing to the Recent Pacific Decadal Variations. *Geophys. Res. Lett.* **45**, 7084–7092 (2018). doi: 10.1029/2018GL079033
63. S. McGregor, M. Khodri, N. Maher, M. Ohba, F. S. R. Pausata, S. Stevenson, in *El Nino Southern Oscillation in a Changing Climate*, M. McPhaden, A. Santoso, W. Cai, Eds. (Wiley, 2020), pp. 267–287.

64. V. M. Mehta, H. Wang, K. Mendoza, Simulations of three natural decadal climate variability phenomena in CMIP5 experiments with the UKMO HadCM3, GFDL-CM2.1, NCAR-CCSM4, and MIROC5 global earth system models. *Clim. Dyn.* **51**, 1559–1584 (2018). doi: 10.1007/s00382-017-3971-8
65. N. Maher, A. S. Gupta, M. H. England, Drivers of decadal hiatus periods in the 20th and 21st centuries. *Geophys. Res. Lett.* **41**, 5978–5986 (2014). doi: 10.1002/2014GL060527
66. G. A. Meehl, J. M. Arblaster, K. Matthes, F. Sassi, H. van Loon, Amplifying the Pacific climate system response to a small 11-year solar cycle forcing. *Science* **325**, 1114–1118 (2009). doi: 10.1126/science.1172872; pmid: 19713524
67. T. Chen *et al*., Coral-Derived Western Pacific Tropical Sea Surface Temperatures During the Last Millennium. *Geophys. Res. Lett.* **45**, 3542–3549 (2018). doi: 10.1002/2018GL077619
68. G. Wang, S. B. Power, S. Mcgree, Unambiguous warming in the western tropical Pacific primarily caused by anthropogenic forcing. *Int. J. Climatol.* **36**, 933–944 (2016). doi: 10.1002/joc.4395
69. E. Weller *et al*., Human-caused Indo-Pacific warm pool expansion. *Sci. Adv.* **2**, e1501719 (2016). doi: 10.1126/sciadv.1501719; pmid: 27419228
70. C. Sun *et al*., Western tropical Pacific multidecadal variability forced by the Atlantic multidecadal oscillation. *Nat. Commun.* **8**, 15998 (2017). doi: 10.1038/ncomms15998; pmid: 28685765
71. K. M. Grise *et al*., Recent tropical expansion: Natural variability or forced response? *J. Clim.* **32**, 1551–1571 (2019). doi: 10.1175/JCLI-D-18-0444.1
72. G. Beaugrand *et al*., Prediction of unprecedented biological shifts in the global ocean. *Nat. Clim. Chang.* **9**, 237–243 (2019). doi: 10.1038/s41558-019-0420-1
73. B. Jebri *et al*., Contributions of internal variability and external forcing to the recent trends in the southeastern pacific and peru-chile upwelling system. *J. Clim.* **33**, 10555–10578 (2020). doi: 10.1175/JCLI-D-19-0304.1
74. A. G. Pendergrass, R. Knutti, F. Lehner, C. Deser, B. M. Sanderson, Precipitation variability increases in a warmer climate. *Sci. Rep.* **7**, 17966 (2017). doi: 10.1038/s41598-017-17966-y; pmid: 29269737
75. G. A. Vecchi *et al*., Weakening of tropical Pacific atmospheric circulation due to anthropogenic forcing. *Nature* **441**, 73–76 (2006). doi: 10.1038/nature04744; pmid: 16672967
76. U. K. Heede, A. V. Fedorov, N. J. Burls, Time Scales and Mechanisms for the Tropical Pacific Response to Global Warming: A Tug of War between the Ocean Thermostat and Weaker Walker. *J. Clim.* **33**, 6101–6118 (2020). doi: 10.1175/JCLI-D-19-0690.1
77. M. F. Stuecker *et al*., Strong remote control of future equatorial warming by off-equatorial forcing. *Nat. Clim. Chang.* **10**, 124–129 (2020). doi: 10.1038/s41558-019-0667-6
78. E. S. Chung *et al*., Reconciling opposing Walker circulation trends in observations and model projections. *Nat. Clim. Chang.* **9**, 405–412 (2019). doi: 10.1038/s41558-019-0446-4
79. C. Takahashi, M. Watanabe, Pacific trade winds accelerated by aerosol forcing over the past two decades. *Nat. Clim. Chang.* **6**, 768–772 (2016). doi: 10.1038/nclimate2996
80. L. Dong, M. J. McPhaden, Why has the relationship between Indian and Pacific Ocean decadal variability changed in recent decades? *J. Clim.* **30**, 1971–1983 (2017). doi: 10.1175/JCLI-D-16-0313.1
81. T. Kohyama, D. L. Hartmann, D. S. Battisti, La Niña-like mean-state response to global warming and potential oceanic roles. *J. Clim.* **30**, 4207–4225 (2017). doi: 10.1175/JCLI-D-16-0441.1
82. A. C. Clement, R. Seager, M. A. Cane, S. E. Zebiak, An ocean dynamical thermostat. *J. Clim.* **9**, 2190–2196 (1996). doi: 10.1175/1520-0442(1996)009<2190:AODT>2.0.CO;2
83. R. Seager *et al*., Strengthening tropical Pacific zonal sea surface temperature gradient consistent with rising greenhouse gases. *Nat. Clim. Chang.* **9**, 517–522 (2019). doi: 10.1038/s41558-019-0505-x
84. J. J. Luo, G. Wang, D. Dommenget, May common model biases reduce CMIP5's ability to simulate the recent Pacific La Niña-like cooling? *Clim. Dyn.* **50**, 1335–1351 (2018). doi: 10.1007/s00382-017-3688-8
85. N. Bellouin *et al*., Bounding Global Aerosol Radiative Forcing of Climate Change. *Rev. Geophys.* **58**, RG000660 (2020). doi: 10.1029/2019RG000660; pmid: 32734279
86. J. Emile-Geay, K. M. Cobb, J. E. Cole, M. Elliot, F. Zhu, in *El Niño Southern Oscillation in a Changing Climate*, M. J. McPhaden, A. Santoso, W. Cai, Eds. (Wiley, 2020), pp. 87–118.
87. P. N. DiNezio *et al*., A 2 Year Forecast for a 60–80% Chance of La Niña in 2017–2018. *Geophys. Res. Lett.* **44**, 11624–11635 (2017). doi: 10.1002/2017GL074904
88. A. A. Scaife, D. Smith, A signal-to-noise paradox in climate science. *NPJ Clim. Atmos. Sci.* **1**, 28 (2018). doi: 10.1038/s41612-018-0038-4
89. D. M. Smith *et al*., Robust skill of decadal climate predictions. *NPJ Clim. Atmos. Sci.* **2**, 13 (2019). doi: 10.1038/s41612-019-0071-y
90. R. Séférian *et al*., Multiyear predictability of tropical marine productivity. *Proc. Natl. Acad. Sci. U.S.A.* **111**, 11646–11651 (2014). doi: 10.1073/pnas.1315855111; pmid: 25071174
91. N. S. Lovenduski, S. G. Yeager, K. Lindsay, M. C. Long, Predicting near-term variability in ocean carbon uptake. *Earth Syst. Dyn.* **10**, 45–57 (2019). doi: 10.5194/esd-10-45-2019
92. Y. Chikamoto, T. Mochizuki, A. Timmermann, M. Kimoto, M. Watanabe, Potential tropical Atlantic impacts on Pacific decadal climate trends. *Geophys. Res. Lett.* **43**, 7143–7151 (2016). doi: 10.1002/2016GL069544
93. G. A. Meehl, H. Teng, CMIP5 multi-model hindcasts for the mid-1970s shift and early 2000s hiatus and predictions for 2016–2035. *Geophys. Res. Lett.* **41**, 1711–1716 (2014). doi: 10.1002/2014GL059256
94. M. Thoma, R. J. Greatbatch, C. Kadow, R. Gerdes, Decadal hindcasts initialized using observed surface wind stress: Evaluation and prediction out to 2024. *Geophys. Res. Lett.* **42**, 6454–6461 (2015). doi: 10.1002/2015GL064833
95. G. A. Meehl, A. Hu, H. Teng, Initialized decadal prediction for transition to positive phase of the Interdecadal Pacific Oscillation. *Nat. Commun.* **7**, 11718 (2016). doi: 10.1038/ncomms11718; pmid: 27251760
96. N. A. Rayner *et al*., Global analyses of SST, sea ice, and night marine air temperature since the late nineteenth century. *J. Geophys. Res.* **108**, 4407 (2003). doi: 10.1029/2002JD002670
97. M. A. Balmaseda, K. Mogensen, A. T. Weaver, Evaluation of the ECMWF ocean reanalysis system ORAS4. *Q. J. R. Meteorol. Soc.* **139**, 1132–1161 (2013). doi: 10.1002/qj.2063
98. E. de Boisséson, M. A. Balmaseda, M. Mayer, Ocean heat content variability in an ensemble of twentieth century ocean reanalyses. *Clim. Dyn.* **50**, 3783–3798 (2018). doi: 10.1007/s00382-017-3845-0
99. G. P. Compo *et al*., The Twentieth Century Reanalysis Project. *Q. J. R. Meteorol. Soc.* **137**, 1–28 (2011). doi: 10.1002/qj.776
100. P. Poli *et al*., ERA-20C: An Atmospheric Reanalysis of the Twentieth Century. *J. Clim.* **29**, 4083–4097 (2016). doi: 10.1175/JCLI-D-15-0556.1

ACKNOWLEDGMENTS

This paper is an initiative of the CLIVAR Pacific Region Panel. We thank J. Li at the World Climate Research Programme (WCRP) Office for helping to organize workshops to help advance this review, the first at Centro Nacional de Acuiccultura e Investigaciones Marinas (CENAIM) and Escuela Superior Politecnica del Litoral (ESPOL) in Ecuador and the second at LOCEAN-IPSL, Sorbonne University in Paris; V. Kharin and G. Boer for providing the data used in Fig. 6A; G. Liguori and J. Crétat for reviewing earlier drafts; P. Bracannot for discussions regarding paleoclimate; R. Séférian for discussions regarding biogeochemistry; and L. Crosswell for finalizing the summary figure. Thanks also to anonymous reviewers for their very helpful and constructive comments. **Funding:** S.P., W.C., F.D., and C.C. were partially supported by the Earth System and Climate Change Hub of the Australian National Environmental Science Programme. W.C., G.W., and X.Z. were supported by the Centre for Southern Hemisphere Oceans Research, a joint research center between QNLM and CSIRO. M.L., J.V., and E.G. were supported by the Agence Nationale de la Recherche ARISE project, under grant ANR-18-CE01-0012; the Belmont project GOTHAM, under grant ANR-15-JCLI-0004-01; and the Make Our Planet Great Again project ARCHANGE, under grant ANR-18-MPGA-0001. A.C. was supported by the NOAA Climate Program Office's Climate Variability and Predictability (CVP) and Modeling, Analysis, Predictions and Projections (MAPP) programs. S.M. was supported by the Australian Research Council through grant FT160100162 and DP200102329. M.C. was supported by the UK's Natural Environment Research Council, grants NE/N018486/1 and NE/N005783/1. This is PMEL contribution no. 5031. G.M. was partially supported by the Regional and Global Model Analysis (RGMA) component of the Earth and Environmental System Modeling Program of the US Department of Energy's Office of Biological and Environmental Research through National Science Foundation (NSF) IA 1844590 and by NCAR, which is a major facility sponsored by the NSF under cooperative agreement no. 1852977. S.M. was supported by the Australian Research Council through grant FT160100162 and DP20. Y.O. was supported by the NOAA Climate Program Office's MAPP program (NA17OAR4310149) and the NSF Physical Oceanography Program (OCE-1756883). M.N. was partially supported by US Department of Energy grant no. 0000238382. J.J.L. was supported by the National Natural Science Foundation of China (grants 42088101 and 42030605). D.S. was supported by the Met Office Hadley Centre Climate Programme funded by BEIS and DEFRA. J.-S.K. was supported by the National Research Foundation of Korea (NRF-2018R1A5A1024958). J.S. was supported by NOAA's Global Ocean Monitoring and Observing Program through award NA20OAR4320278. B.J.H. was supported by an Australian Research Council Linkage Project (LP150100062). **Author contributions:** The manuscript was drafted as a group effort during two specially convened workshops attended by nearly all co-authors. All authors contributed to the manuscript preparation, interpretations, and the discussions that led to the final draft. S.P., A.C., and M.L. led the discussions and coordinated the analysis and writing, with M.L. leading finalization of Figs. 1 to 5. S.P. drafted the summary figure. S.P., M.L., A.C., M.K., J.V., S.M., and G.M. coordinated discussions and writing of subsections; J.-S.K., G.-I.K., M.K., D.V., B.J., J.E.-G., S.M., C.C., and F.D. provided analyses and/or helped with figures. **Competing interests:** The authors declare no competing interests. **Data and materials availability:** All observational and model datasets used here are publicly available or available on request.

10.1126/science.aay9165

Decadal climate variability in the tropical Pacific: Characteristics, causes, predictability, and prospects

Scott Power, Matthieu Lengaigne, Antonietta Capotondi, Myriam Khodri, Jérôme Vialard, Beyrem Jebri, Eric Guilyardi, Shayne McGregor, Jong-Seong Kug, Matthew Newman, Michael J. McPhaden, Gerald Meehl, Doug Smith, Julia Cole, Julien Emile-Geay, Daniel Vimont, Andrew T. Wittenberg, Mat Collins, Geon-Il Kim, Wenju Cai, Yuko Okumura, Christine Chung, Kim M. Cobb, François Delage, Yann Y. Planton, Aaron Levine, Feng Zhu, Janet Sprintall, Emanuele Di Lorenzo, Xuebin Zhang, Jing-Jia Luo, Xiaopei Lin, Magdalena Balmaseda, Guojian Wang, and Benjamin J. Henley

Science **374** (6563), eaay9165. DOI: 10.1126/science.aay9165

A decades-long affair

Decadal climate variability and change affects nearly every aspect of our world, including weather, agriculture, ecosystems, and the economy. Predicting its expression is thus of critical importance on multiple fronts. Power *et al*. review what is known about tropical Pacific decadal climate variability and change, the degree to which it can be simulated and predicted, and how we might improve our understanding of it. More accurate projections will require longer and more detailed instrumental and paleoclimate records, improved climate models, and better data assimilation methods. —HJS